1-1994

Regulation of intracellular cyclic GMP concentration by light and calcium in electropermeabilized rod photoreceptors.

V J. Coccia
University of New Hampshire - Main Campus

Rick H. Cote
University of New Hampshire - Main Campus, rick.cote@unh.edu

Recommended Citation
Coccia, V.J., Cote, R.H. Regulation of intracellular cyclic GMP concentration by light and calcium in electropermeabilized rod photoreceptors. (1994) Journal of General Physiology, 103 (1), pp. 67-86. doi: 10.1085/jgp.103.1.67.

Onset of Feedback Reactions Underlying Vertebrate Rod Photoreceptor Light Adaptation

Peter D. Calvert,* Theresa W. Ho,‡ Yvette M. LeFebvre,* and Vadim Y. Arshavsky*

From the *Howe Laboratory of Ophthalmology, Harvard Medical School and the Massachusetts Eye and Ear Infirmary, Boston, Massachusetts 02114; and ‡Laboratory of Molecular Biology, University of Wisconsin, Madison, Wisconsin 53706

abstract Light adaptation in vertebrate photoreceptors is thought to be mediated through a number of biochemical feedback reactions that reduce the sensitivity of the photoreceptor and accelerate the kinetics of the photoresponse. Ca^{2+} plays a major role in this process by regulating several components of the phototransduction cascade. Guanylate cyclase and rhodopsin kinase are suggested to be the major sites regulated by Ca^{2+}. Recently, it was proposed that cGMP may be another messenger of light adaptation since it is able to regulate the rate of transducin GTPase and thus the lifetime of activated cGMP phosphodiesterase. Here we report measurements of the rates at which the changes in Ca^{2+} and cGMP are followed by the changes in the rates of corresponding enzymatic reactions in frog rod outer segments. Our data indicate that there is a temporal hierarchy among reactions that underlie light adaptation. Guanylate cyclase activity and rhodopsin phosphorylation respond to changes in Ca^{2+} very rapidly, on a subsecond time scale. This enables them to accelerate the falling phase of the flash response and to modulate flash sensitivity during continuous illumination. To the contrary, the acceleration of transducin GTPase, even after significant reduction in cGMP, occurs over several tens of seconds. It is substantially delayed by the slow dissociation of cGMP from the noncatalytic sites for cGMP binding located on cGMP phosphodiesterase. Therefore, cGMP-dependent regulation of transducin GTPase is likely to occur only during prolonged bright illumination.

key words: light adaptation • guanylate cyclase • phosphodiesterase • rhodopsin kinase • Ca^{2+}

introduction

Photoresponses in vertebrate photoreceptors begin when light activates an enzymatic cascade including rhodopsin, transducin, and phosphodiesterase (PDE).[1] The resulting decrease in cGMP causes closure of cationic channels in the plasma membrane of the photoreceptor outer segment (reviewed in Chabre and Deterre, 1989; Pugh and Lamb, 1990). Photoreceptors adapt to ambient light through feedback reactions that regulate either the catalytic activity or the catalytic lifetime of individual components of the phototransduction cascade. It is well established that Ca^{2+} plays a significant role in this process (reviewed by Lagnado and Baylor, 1992; Koutalos and Yau, 1993; Bownds and Arshavsky, 1995). Ca^{2+} declines in response to light because it can no longer enter through the cationic channels while it continues to be extruded through the Na/Ca,K exchanger. There are at least three sites of Ca^{2+} regulation in the cascade. The first is the regulation of the lifetime of light-activated rhodopsin. Rhodopsin is turned off when it is phosphorylated by rhodopsin kinase followed by the binding of arrestin. Rhodopsin phosphorylation is inhibited when rhodopsin kinase forms a complex with the Ca^{2+}-binding protein, recoverin. The light-dependent decrease in cytoplasmic Ca^{2+} is thought to cause the dissociation of this complex, increasing the rate of rhodopsin phosphorylation. Another site of Ca^{2+} regulation is guanylate cyclase, the enzyme responsible for cGMP synthesis. This regulation is conferred through the Ca^{2+} binding proteins known as guanylate cyclase activating proteins (GCAPs) (Palczewski et al., 1994; Dizhoon et al., 1995). Cyclase activity is low in darkness and increases when Ca^{2+} levels drop in response to light. The third site is the regulation of the sensitivity of the cationic channel to cGMP. Lowering Ca^{2+} causes the channel to become more sensitive to cGMP due to the dissociation of calmodulin (CaM) or a closely related Ca^{2+} binding protein. This might result in the accelerated recovery of the photoresponse by facilitating the reopening of channels. In addition, the gain of the cascade may also be regulated by Ca^{2+} independently of changes in inactivation and recovery (Lagnado and Baylor, 1994). This hypothesis is based on the observation that the rate of the photoresponse rising phase in truncated rods is reduced when Ca^{2+} concentration is lowered.

cGMP might also serve as a messenger of adaptation by regulating the duration of PDE activation by transducin (Arshavsky et al., 1991, 1992; Arshavsky and Bownds,

Address correspondence to Peter D. Calvert, Howe Laboratory/MEEI, 243 Charles St., Boston, MA 02114. Fax: 617-573-4290; E-mail: pdcalvert@meei.harvard.edu

[1]*Abbreviations used in this paper:* CaM, calmodulin; PDE, rod photoreceptor cGMP-phosphodiesterase; ROS, rod outer segment.

1992; Cote et al., 1994). cGMP binding to noncatalytic sites on the PDE molecule modulates the rate of transducin GTPase, the reaction responsible for PDE shut off. When these sites are occupied by cGMP, the rate of GTP hydrolysis is relatively slow and thus PDE stays active for a relatively long time. When light causes the decline of free cGMP, followed by cGMP dissociation from the noncatalytic sites, the rate of GTP hydrolysis is accelerated by severalfold and the duration of PDE activation is reduced. This mechanism could accelerate the recovery of the photoresponse.

To understand the time course of the onset of the feedback controls discussed above, three issues should be addressed: (*a*) the kinetic parameters for the regulation of the enzymes targeted by feedback messengers, (*b*) the rate of reduction of free feedback messengers in the photoreceptor cytoplasm in response to light, and (*c*) the delay between feedback messenger decline and the corresponding change in enzymatic activity (including the dissociation of bound messengers from regulatory proteins and the subsequent change in protein–protein interactions). The rates of cGMP and Ca^{2+} reductions in rod outer segments (ROS) have been well characterized. Changes in free cGMP are simply reflected in the changes in the photocurrent that senses cGMP concentration with only a millisecond delay (reviewed by Yau and Baylor, 1989). Changes in free Ca^{2+} have been studied by a number of laboratories (McCarthy et al., 1994, 1996; Gray-Keller and Detwiler, 1994; Younger et al., 1996; Sampath et al., 1997). Ca^{2+} decline with light in frog, gecko, and salamander photoreceptors is described as the sum of at least two exponential processes, one with a subsecond time constant and another with a time constant of several seconds. Practically nothing is known about the delay between Ca^{2+} and cGMP decline and the changes in corresponding enzymatic activities. Physiological experiments have indirectly addressed some of these questions, but few have been approached in direct biochemical experiments.

Our goal was to study how fast the reduction in free Ca^{2+} results in the stimulation of guanylate cyclase activity and the disinhibition of rhodopsin kinase and how fast the reduction in free cGMP results in the acceleration of transducin GTPase rate. Bullfrogs were selected as an experimental animal because all three of these feedback reactions exist in their rods, frog ROS can be obtained in a quantity sufficient for biochemical experiments and it is one of only three species where the changes in intracellular free Ca^{2+} are described in detail. We have found that the Ca^{2+}-dependent increase in the activities of rhodopsin kinase and guanylate cyclase occur very quickly, on a time scale of a few hundred milliseconds. This indicates that the regulation of these enzymes takes place on the time frame of the Ca^{2+} change in photoreceptor cytoplasm. In contrast, changes in transducin GTPase activity do not directly follow the decline of free cGMP, but are delayed for several tens of seconds due to the slow dissociation of cGMP from PDE noncatalytic cGMP binding sites.

METHODS

Materials

[8-^{3}H]cGMP, [γ-^{32}P]GTP, [α-^{33}P]GTP, and [γ-^{32}P]ATP were purchased from Du Pont-NEN (Boston, MA), Percoll from Pharmacia LKB Biotechnology Inc. (Piscataway, NJ), potassium isethionate from Eastman Kodak Co. (Rochester, NY), nitrocellulose filters from Whatmann Inc. (Clifton, NJ), and BAPTA and Fluo-3 from Molecular Probes, Inc. (Eugene, OR). All other chemicals were obtained from Sigma Chemical Co. (St. Louis, MO) (CaM-PDE and CaM from bovine brain were product No. P9529 and P2277, respectively).

Solutions

The Ringer's solution used to isolate ROS contained (mM): 105 NaCl, 2 KCl, 2 $MgCl_2$, 1 $CaCl_2$, and 10 HEPES, pH 7.5. The pseudointracellular medium used in all experiments contained 95 mM potassium isethionate, 15 mM sodium isethionate, 5 mM $MgCl_2$, 2 mM dithiothreitol, 10 μM leupeptin, 100 kallikrein U/ml aprotinin, and 10 mM HEPES, pH 7.8. The pseudointracellular medium was passed over a Chelex 100 column before $MgCl_2$ addition in order to remove contaminating Ca^{2+}. All the solutions had a final osmolarity of 232–238 mosM. Where required, Ca^{2+} in the pseudointracellular medium was buffered by BAPTA as described in Klenchin et al. (1995). Since commercially available $CaCl_2$ and BAPTA salts contain unpredictable levels of H_2O, which could significantly affect their concentrations on making stock solutions, the H_2O content in these salts was determined gravimetrically and their formula weights were adjusted accordingly. 4× stock solutions with varying concentrations of $CaCl_2$ and 20 mM BAPTA concentration were prepared in the pseudointracellular medium. Free Ca^{2+} concentrations of these stocks were calculated using the program BAD (Brooks and Story, 1992). The validity of this method was checked using both a calcium selective electrode (Microelectrodes, Inc., Londonderry, NH) and Fluo-3 indicator dye.

Preparation of Rod Outer Segments

Live bullfrogs (*Rana catesbeiana* or *Rana grylio*) were purchased from commercial sources and maintained with feeding on a 12-h light–dark cycle for at least 2 wk before use (Woodruff and Bownds, 1979). All manipulations were performed under infrared illumination. Animals were killed by decapitation, retinas were removed, placed into Ringer solution containing 5% Percoll, and ROS were purified on a Percoll gradient as described in Biernbaum and Bownds (1985*a*). Intact ROS were washed free of Percoll in pseudointracellular medium and kept on ice. Before each experiment, ROS were disrupted in a Potter-Elvehjem homogenizer, creating a membrane suspension with no structure detectable under light microscopy (Dumke et al., 1994). Rhodopsin concentration was determined spectrophotometrically according to Bownds et al. (1971). All experiments were carried out at 22°C.

Guanylate Cyclase Assay

Guanylate cyclase activity was determined in ROS homogenates using thin layer chromatography as described by Dizhoor et al.

(1994). The reaction was performed in 500 μl Eppendorf tubes upon vigorous vortexing. The reaction was started by the addition of 10 μl of pseudointracellular medium supplemented with [α-^{33}P]GTP (either 1 mM or 200 μM), 10 μM ATP, and 10 mM [^{3}H]cGMP to 10 μl of the ROS suspension supplemented with 100 μM zaprinast and Ca^{2+}-BAPTA buffer. ^{33}P-labeled GTP, ATP, and zaprinast were used to reduce PDE activity that would otherwise hydrolyze the cGMP formed by guanylate cyclase, confounding the measurement of its activity. ^{33}P-labeled GTP was used rather than ^{32}P-GTP to avoid bleaching of rhodopsin by Cerenkov radiation, caused by the decay of $^{32}P_i$, and the subsequent activation of PDE (Biernbaum et al., 1991). ATP was provided to quench contaminating bleached rhodopsin in the preparation through its phosphorylation by endogenous kinase. Zaprinast is a potent PDE inhibitor (Gillespie and Beavo, 1989). This strategy reduced the hydrolysis of cGMP, as measured by the reduction in added [^{3}H]cGMP, to <5% over the time course of our experiments. The reaction was quenched with 100 μl of 50 mM EDTA, pH 7.0, followed by 1 min boiling to precipitate proteins. Samples were then centrifuged on a Beckman Microfuge E for 10 min and 10-μl aliquots were loaded on PEI-cellulose thin layer chromatography plates (EM Sciences, Gibbstown, NJ). The nucleotides were separated using 0.2 M LiCl. Spots containing cGMP were visualized under ultraviolet illumination, cut from the plate, eluted with 2 M LiCl, mixed with 10 ml ScintiSafe cocktail (Fisher Scientific Co., Santa Clara, CA) and counted in a scintillation counter.

Rhodopsin Phosphorylation Assay

Rhodopsin phosphorylation was measured essentially as described by Klenchin et al. (1995). The reaction was started with the addition 10 μl of [γ-^{32}P]ATP to 10 μl ROS containing Ca^{2+}-BAPTA buffer and 30 μM myristoylated recombinant bovine recoverin. The reaction was quenched with 80 μl of 50 mM EDTA, 100 mM KF, and 100 mM Na-phosphate buffer, pH 7.5. This solution terminated both rhodopsin phosphorylation and dephosphorylation. 50 μl of quenched sample was applied to nitrocellulose filter and washed six times with 1 ml of 100-mM Na-phosphate buffer, pH 7.5. Filters were placed in scintillation vials, dissolved in 2 ml glacial acetic acid, mixed with 10 ml ScintiSafe (Fisher Scientific Co.) and counted. Recombinant recoverin was produced using a bacterial expression system (Dizhoor et al., 1993). The expression system was a kind gift from Dr. J.B. Hurley (University of Washington, Seattle, WA).

cGMP Binding Assay

cGMP binding to the PDE noncatalytic sites was determined by the nitrocellulose filter binding technique described in detail by Cote and Brunnock (1993). ROS were incubated for 30 min at room temperature to completely dissociate the endogenous cGMP from the PDE noncatalytic sites. Nucleotide-depleted ROS were incubated for 1 min with 3 μM [^{3}H]cGMP, a time sufficient to reach binding equilibrium (Cote and Brunnock, 1993). Dissociation of the labeled cGMP was then initiated by a chase with either an excess of the unlabeled cGMP or a mixture of CaM-PDE with CaM (80 U CaM per unit CaM-PDE). At different times after the chase, 15-μl portions were added to nitrocellulose filters. The filters were rinsed with three 1-ml portions of ice-cold pseudointracellular medium, dissolved in glacial acetic acid and counted in ScintiSafe cocktail.

GTPase Assay

Transducin GTPase activity was determined by a modified method of Godchaux and Zimmerman (1979) described by Arshavsky et al. (1991). 20 μl of bleached ROS (20 μM rhodopsin final concentration) were mixed with 10 μl of [γ-^{32}P]GTP (4 μM final concentration) in 1.5 ml Eppendorf tubes. The reaction was stopped in 3 s with 100 μl of 6% perchloric acid. The samples were incubated for 10 min with 0.7 ml activated charcoal (100 mg/ml in 50 mM Na-phosphate buffer, pH 7.5), sedimented, and $^{32}P_i$ in the supernatant was measured with ScintiSafe cocktail. Control experiments carried out in darkness indicate that >90% of GTP hydrolysis was light-dependent. Therefore, we conclude that most of the GTPase activity in these experiments is attributable to transducin.

RESULTS

Ca^{2+} Feedback

Guanylate cyclase activity changes quickly after a rapid change in free Ca^{2+}. The regulation of guanylate cyclase activity by Ca^{2+} in rod photoreceptor outer segments has been well characterized in bovine rod photoreceptors (Koch and Stryer, 1988; Gorczyca et al., 1994*b*; Dizhoor et al., 1994). Ca^{2+} regulation of the guanylate cyclase in frog ROS has also been established (Coccia and Cote, 1994); however, a detailed analysis of the Ca^{2+} dependence was not performed. Such an analysis in a suspension of

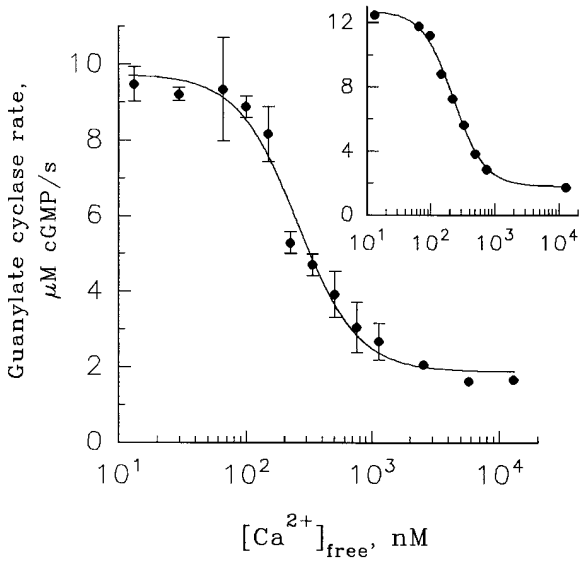

FIGURE 1. Ca^{2+} dependence of frog ROS guanylate cyclase activity. The cyclase reaction was initiated by adding 10 μl of pseudointracellular medium containing 2 mM [γ-^{33}P]GTP, 20 μM ATP, 20 mM [^{3}H]-cGMP, and Ca^{2+} buffered to indicated concentration to 10 μl of a ROS suspension containing 40 μM rhodopsin and 200 μM zaprinast buffered to the same Ca^{2+}. After 30 s, the reaction was stopped with the addition of 80 μl of a quench solution containing 50 mM EDTA, pH 7.0. The cyclase activity is expressed as μM cGMP produced in the equivalent ROS cytoplasm per second and is plotted against the free Ca^{2+} concentration. Each point represents the mean ± SD of four separate determinations. The solid line is a fit of Eq. 1 to the data with α_{max} = 9.74, α_{min} = 1.88, $K_{1/2}$ = 256 nM Ca^{2+}, and n = 1.82. (*inset*) A similar experiment carried out at 180 μM rhodopsin. Here, fitting Eq. 1 to the data gave α_{max} = 12.7, α_{min} = 1.8, $K_{1/2}$ = 230 nM Ca^{2+}, and n = 1.85.

frog ROS is shown in Fig. 1. The cyclase activity was expressed as the cGMP concentration produced in the ROS cytoplasm per second. The value of 6 mM rhodopsin with respect to the ROS cytoplasm was used (see Bownds and Arshavsky, 1995). The Ca^{2+} dependence was approximated by the Hill equation:

$$\alpha = \alpha_{max} - (\alpha_{max} - \alpha_{min}) \cdot \frac{Ca^n}{Ca^n + K_{1/2}^n} \quad (1)$$

where α is the rate of cGMP formation, α_{max} is the maximum cyclase rate at low Ca^{2+}, α_{min} is the minimum cyclase rate at high Ca^{2+}, $K_{1/2}$ is the half saturating Ca^{2+} concentration, and n is the Hill coefficient. Fitting this equation to the data in Fig. 1, accumulated in four independent experiments performed in a ROS suspension containing 20 μM rhodopsin, yielded α_{max} = 9.74 ± 0.4 μM/s (mean ± SD), α_{min} = 1.9 ± 0.2 μM/s with $K_{1/2}$ = 255 ± 21 nM and n = 1.8 ± 0.2. These values are similar to those found for rod cells of other vertebrate species (Koch and Stryer, 1988; Gorczyca et al., 1994*a*; Dizhoor et al., 1994; Koutalos et al., 1995*a*). Since it has been reported that ATP and its nonhydrolyzable analogs stimulate the activity of guanylate cyclase in other systems (Gorczyca et al., 1994*b*; Aparicio and Applebury, 1996), we tested whether ATP has a similar effect in our preparation. No effect of ATP was observed (not shown), probably because ATP does not dissociate from corresponding regulatory sites in a fresh suspension of frog ROS.

In the next set of experiments, we determined whether the parameters of the Ca^{2+}-dependent cyclase regulation are dependent on the ROS concentration used in the assay. While $K_{1/2}$ and n are essentially unaffected, the magnitude of the effect is higher at high than at low ROS concentrations (see Fig. 1, *inset*). A more thorough investigation of the ROS concentration effect on the extent of cyclase regulation by Ca^{2+} is shown in Fig. 2, where the cyclase rates at low and high Ca^{2+} were measured at various concentrations of ROS taken from the same stock. The increase in ROS concentration is accompanied by both an increase of cyclase activity at low Ca^{2+} and a decrease in cyclase activity at high Ca^{2+} (Fig. 2 *A*). This result is consistent with a larger fraction of cyclase being in a complex with guanylate cyclase–activating protein, which, according to Dizhoor and Hurley (1996), serves both as cyclase activator at low Ca^{2+} and cyclase inhibitor at high Ca^{2+}. As shown in Fig. 2 *B*, the highest ratio that we observed was ~10-fold. This effect does not saturate over the range of ROS concentration that we could study, precluding us from providing the exact magnitude of this regulation in intact frog ROS.

Next we measured how rapidly the cyclase activity increased after Ca^{2+} was abruptly changed from high to low concentration. ROS suspensions were preincubated either at 10 μM or 10 nM Ca^{2+} for at least 2 min before the initiation of the cyclase reaction. The reaction was initiated by the addition of [α-^{33}P]GTP according to one of three protocols: (*a*) Ca^{2+} was high throughout the experiment—ROS suspensions containing 10 μM Ca^{2+} were mixed with medium containing [α-^{33}P]GTP and 10 μM Ca^{2+}; (*b*) Ca^{2+} was low throughout the experiment—ROS suspensions containing 10 nM Ca^{2+} were mixed with medium containing [α-^{33}P]GTP and 10 nM Ca^{2+}; and (*c*) Ca^{2+} started high and was lowered at the initiation of the reaction—

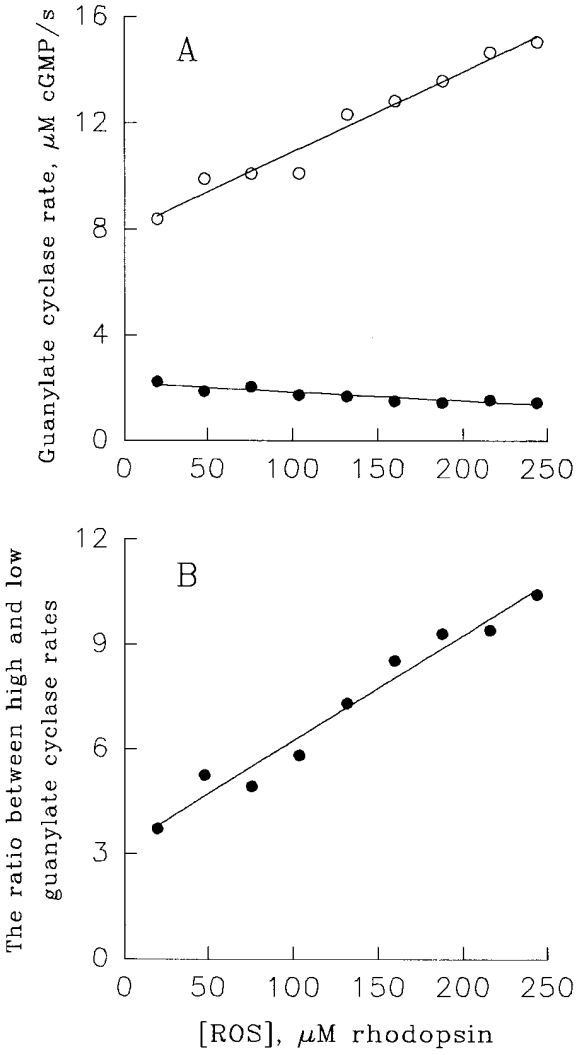

FIGURE 2. The extent of Ca^{2+}-dependent regulation of guanylate cyclase activity in frog ROS increases with the increase in ROS concentration. (*A*) The cyclase activity in ROS suspensions containing indicated amounts of rhodopsin was measured at 13 nM (○) and 13 μM (●) Ca^{2+} as described for Fig. 1, except that 1 mM GTP was used and the incubation time was 20 s. The lines represent linear regression drawn through the points. (*B*) The ratios of values obtained in *A* for low and high Ca^{2+} are plotted as a function of ROS concentration. The line is a linear regression drawn through the points. All data are taken from one of three identical experiments.

ROS suspensions containing 10 μM Ca^{2+} were mixed with medium containing [α-^{33}P]GTP and 1 mM EGTA, an amount sufficient to reduce the Ca^{2+} concentration to 10 nM (we will refer to this protocol as the transition condition). To improve the signal to noise ratio in these experiments, we used 200 μM GTP, close to the cyclase K_m value. Fig. 3 *A* shows the synthesis of cGMP under each of the three conditions. In each case, cGMP synthesis was practically a linear process and the cyclase activity measured under the transition condition was essentially equal to the rate measured under the low Ca^{2+} condition. A more precise analysis of the data obtained under the transition condition was performed with the following equation:

$$\text{cGMP} = \alpha_{min} \cdot t + (\alpha_{max} - \alpha_{min}) \cdot \int_0^t (1 - e^{-t/\tau})\, dt \quad (2)$$

where τ is the time constant for the exponential transition of the cyclase rate from α_{min} to α_{max} after a sudden reduction in Ca^{2+}. The mean value of α from three experiments was ~200 ms. The dashed line in Fig. 3, which represents a theoretical transition with τ = 1 s, provides a measure of the resolution of this technique. τ in this experiment includes the time constant for the dissociation of Ca^{2+} from its binding sites on the guanylate cyclase regulatory proteins and any subsequent physical processes that lead to a change in the cyclase rate as well as the experimentally introduced delay associated with the mixing of reactants. Therefore, the τ obtained using this analysis should be considered as an upper limit for the cyclase transition.

Using a similar strategy, we also analyzed how rapidly the cyclase activity decreased after Ca^{2+} was abruptly increased. The choice of Ca^{2+} range in this experiment was more crucial than in the previous experiment because the rate of Ca^{2+} binding to the cyclase regulatory proteins is a function of free Ca^{2+} concentration, whereas the rate of Ca^{2+} dissociation in the previous experiment is not. Thus, the 100–500-nM Ca^{2+} step was selected because it covered most of the dynamic range of cyclase regulation and most of the physiological range of Ca^{2+} changes. Fig. 3 *B* shows that the decrease

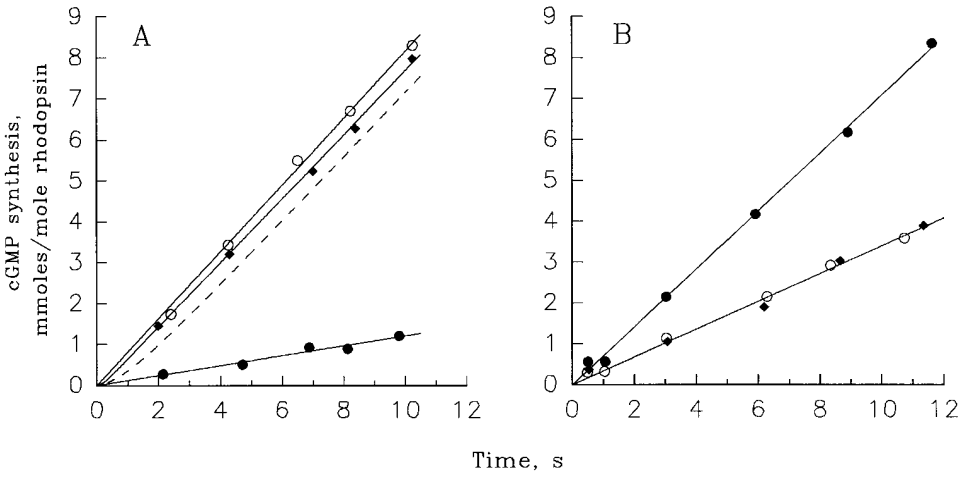

FIGURE 3. Guanylate cyclase activity quickly changes after a rapid change in free Ca^{2+}. (*A*) The transition from slow to fast cyclase rate. The time course of cGMP synthesis in ROS suspensions containing 20 μM rhodopsin was measured with 10 μM Ca^{2+} (●), 10 nM Ca^{2+} (○), and after a step from 10 μM to 10 nM Ca^{2+} (◆). The cyclase reaction was initiated with the addition of 10 μl pseudointracellular medium containing 400 μM [α-^{33}P]GTP and 20 mM cGMP to 10 μl of ROS suspensions containing 40 μM rhodopsin and 200 μM zaprinast. At indicated times, the reaction was quenched with 80 μl of 50 mM EDTA, pH 7.0. The data are plotted as the millimoles cGMP produced per mole of rhodopsin versus time. The solid lines through the closed and open circles are straight lines originating from zero, providing cyclase rates of 0.72 and 4.92 μM/s, respectively. The solid line through the diamonds is a fitting of Eq. 2 to the data where α_{min} = 0.72 μM/s, α_{max} = 4.68 μM/s, and τ = 200 ms. The dashed line, provided for comparison, was generated using Eq. 2 setting α_{min} = 0.72 μM/s, α_{max} = 4.68 μM/s, and τ = 1 s. The figure is representative of three similar experiments. (*B*) The transition from fast to slow cyclase rate. An experiment analogous to that shown in *A* was performed to estimate the rate of transition of the cyclase rate at 100 nM Ca^{2+} to that at 500 nM Ca^{2+}. The time course of the cGMP production in ROS suspensions containing 20 μM rhodopsin was measured under three different conditions: (*a*) ROS contained 500 nM Ca^{2+} and stayed at 500 nM Ca^{2+} throughout the experiment (○); (*b*) ROS contained 100 nM Ca^{2+} and stayed at 100 nM Ca^{2+} throughout the experiment (●); and (*c*) ROS were incubated at 100 nM Ca^{2+} before the experiment, and then Ca^{2+} was increased to 500 nM at time zero (◆). The lines through the filled and open circles are straight lines originating from zero, providing cyclase rates of 4.3 and 2.0 μM/s, respectively. The data for the transition condition are fit with Eq 3:

$$\text{cGMP} = \alpha_{500} \cdot t + (\alpha_{100} - \alpha_{500}) \cdot \int_0^t (e^{-t/\tau})\, dt \quad (3)$$

where α_{500} is the cyclase rate at 500 nM Ca^{2+} and α_{100} is the cyclase rate at 100 nM Ca^{2+}. This analysis yielded a τ indistinguishable from zero. The figure shows one of two similar experiments.

in cyclase activity upon Ca^{2+} increase was also very fast (τ less than the resolution of this technique), indicating that the change in the rate of cyclase closely follows the change in intracellular Ca^{2+} concentration in either direction.

Rhodopsin Kinase Activity Increases Quickly after a Rapid Reduction in Free Ca^{2+}. We measured how fast the rhodopsin kinase activity increased when Ca^{2+} was abruptly changed from high to low concentration in experiments similar to those described for the guanylate cyclase. Previous studies have shown that the affinity of recoverin for rhodopsin kinase is low and that significant effects of recoverin on rhodopsin phosphorylation in ROS suspensions may be observed only with the addition of exogenous recoverin (Kawamura, 1993; Klenchin et al., 1995). Therefore, we supplemented ROS suspensions with 30 μM exogenous recoverin, which approximates the endogenous concentration in the cytoplasm of intact frog ROS (Klenchin et al., 1995). We used myristoylated recombinant bovine recoverin, which regulates rhodopsin phosphorylation in frog ROS in the same way as the endogenous frog recoverin (Kawamura et al., 1993; Klenchin et al., 1995). Recoverin-supplemented ROS suspensions were preincubated either at 10 μM or 10 nM Ca^{2+} for at least 2 min before the initiation of the rhodopsin phosphorylation reaction. Rhodopsin was fully bleached with white light immediately before initiation of the reaction to ensure that it is not limiting in the reaction. The reaction was started by the addition of 25 μM [γ-^{32}P]ATP according to one of three protocols (analogous to the cyclase conditions described above): (*a*) ROS in 10 μM Ca^{2+} were mixed with [γ-^{32}P]ATP in 10 μM Ca^{2+}; (*b*) ROS in 10 nM Ca^{2+} were mixed with [γ-^{32}P]ATP in 10 nM Ca^{2+}; (*c*) ROS in 10 μM Ca^{2+} were mixed with [γ-^{32}P]ATP in the pseudointracellular medium containing 1 mM EGTA, an amount sufficient to reduce the Ca^{2+} concentration to 10 nM upon the start of the reaction.

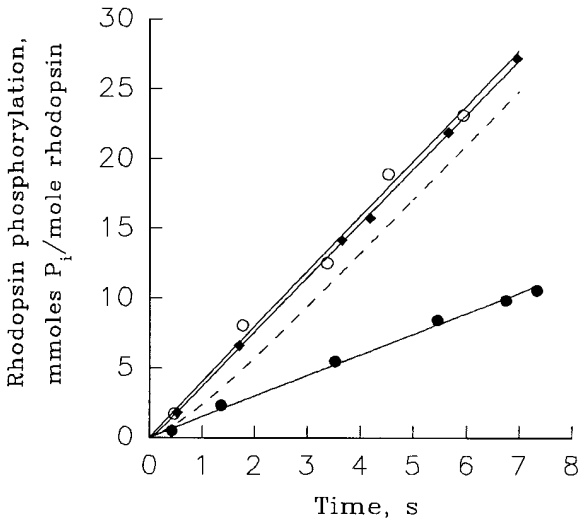

FIGURE 4. Rhodopsin kinase activity quickly increases after a rapid reduction in free Ca^{2+}. The time course of rhodopsin phosphorylation in ROS supplemented with 30 μM myristoylated recombinant recoverin was measured under three different conditions: (*a*) ROS contained high 10-μM Ca^{2+} and stayed at this Ca^{2+} throughout the experiment (●); (*b*) ROS contained 10-nM Ca^{2+} and stayed at this Ca^{2+} throughout the experiment (○); (*c*) ROS were incubated at 10 μM Ca^{2+} before the initiation of the reaction, and then Ca^{2+} was reduced to 10 nM at time zero (◆). The phosphorylation reaction was initiated when 10 μl of pseudointracellular medium containing 50 μM [γ-^{32}P]ATP was added to 10 μl of ROS suspension containing 100 μM rhodopsin and 60 μM myristoylated recoverin. Just before initiating the reaction, ROS suspensions were exposed to bright white light for 30 s to fully bleach the rhodopsin. The reaction was quenched with the addition of 80 μl 50-mM EDTA containing 100 mM KF and 100 mM phosphate buffer, pH 7.5. The data are plotted as millimoles P_i incorporated into rhodopsin per mole rhodopsin versus time. The solid lines through the closed and open circles are straight lines originating from zero, providing rhodopsin phosphorylation rates of 1.46 and 3.94 mmol P_i/mol rhodopsin per second, respectively. The solid line through the diamonds is provided by an analysis similar to that performed in Fig. 3. The minimal phosphorylation rate (analogous to α_{min} in Fig. 3) was 1.46 mmol P_i/mol rhodopsin per second, the maximal phosphorylation rate was 3.94 mmol P_i/mol rhodopsin per second and τ was 110 ms. The dashed line was generated by setting the minimal phosphorylation rate to 1.46 mmol P_i/mol rhodopsin per second, the maximal phosphorylation rate to 3.94 mmol P_i/mol rhodopsin per second and τ to 1 s. The figure is representative of three similar experiments.

As with the cyclase, the incorporation of P_i into rhodopsin measured under the transition condition was essentially equal to the rate measured in the low Ca^{2+} condition (Fig. 4). Using a similar approach as that used for the cyclase, a time constant for the transition between slow and fast rhodopsin phosphorylation of ~100 ms was obtained, which is less than resolution of our method. Measurements of the kinase activity decrease after Ca^{2+} increase were not performed, since the dynamic range of the Ca^{2+}-dependent kinase regulation in vitro, where measurements could be performed, is ~10-fold higher than that predicted in vivo (Klenchin et al., 1995; Chen et al., 1995) and the transition rates obtained at this high Ca^{2+} would not represent the physiological situation.

cGMP Feedback

cGMP dissociation from the PDE noncatalytic sites after a rapid reduction in free cGMP. One goal of this study was to correlate the rate of cGMP dissociation from PDE noncatalytic cGMP binding sites with the dynamics of transition between "slow" and "fast" transducin GTPase measured in the same ROS suspension. To carry out these experiments, we needed to modify the pulse-chase technique previously used for monitoring cGMP dissociation from the noncatalytic sites (Cote and Brunnock, 1993; Cote et al., 1994). In those studies, noncatalytic sites were first loaded with radio-labeled cGMP,

and then its dissociation from the sites was monitored after a chase with a large excess of nonlabeled cGMP. This approach could not be used in this study since the nonlabeled cGMP quickly substitutes labeled cGMP in the noncatalytic sites and, therefore, they remain occupied during the entire course of the experiment. Instead, we needed to rapidly remove free cGMP as well as cGMP dissociating from the noncatalytic sites from the reaction mixture. To accomplish this, we substituted the cGMP chase with the addition of an excess of CaM-PDE from bovine brain, which hydrolyzes free but not bound cGMP. We decided to use CaM-PDE rather than any other phosphodiesterase type because it has a high level of cGMP hydrolytic activity, lacks noncatalytic cGMP binding sites, and is commercially available. CaM-PDE in the chase was fully activated by CaM and $CaCl_2$. Control experiments have shown that Ca^{2+}, CaM, and CaM-PDE do not interfere with GTP hydrolysis by transducin and that addition of Ca^{2+} and CaM does not alter the kinetics of cGMP dissociation from PDE noncatalytic sites as measured by a chase with excess cGMP (data not shown).

The kinetics of cGMP dissociation from the noncatalytic sites of nonactivated PDE after addition of various amounts of CaM/CaM-PDE are shown in Fig. 5 *A*. A suspension of frog ROS was preincubated with 3 μM [^{3}H]cGMP for 1 min, and then, at time zero, either buffer (Fig. 5 *A*, *upper curve*) or indicated amounts of CaM/CaM-PDE were added. The addition of buffer alone causes a very slow reduction in the amount of [^{3}H]cGMP bound to the PDE noncatalytic sites. This process is slow most likely because the probability of dissociated cGMP to rebind with the noncatalytic sites is higher than the probability for this cGMP to be hydrolyzed by the basal PDE activity. Additions of increasing concentrations of CaM/CaM-PDE result in a faster decline of the amount of [^{3}H]cGMP bound to the PDE noncatalytic sites until saturation occurs at CaM-PDE concentration of ~150 activity U/liter. cGMP dissociation at saturating concentrations of CaM-PDE is described as a single exponential process with a rate constant of 0.0032 ± 0.0003 s^{-1} (n = 8), close to the rate constant observed after a chase with excess nonlabeled cGMP (0.0025 ± 0.0002 s^{-1}, n = 3; Fig. 5 *B*).

Transition between slow and fast transducin GTPase directly follows cGMP dissociation from PDE noncatalytic binding sites. The correlation of cGMP dissociation from the PDE noncatalytic sites with the transition between slow and fast transducin GTPase is shown in Fig. 6. Bleached ROS were preincubated with [^{3}H]cGMP to fully occupy the PDE noncatalytic sites, and then the dissociation of bound cGMP was initiated at time zero by a chase with CaM/CaM-PDE. Aliquots were taken from this mixture to determine either the amount of bound cGMP (Fig. 6 *A*) or the rate of transducin GTPase (Fig. 6 *B*). The GTPase determinations were initiated with the addition of either [γ-^{32}P]GTP or a mixture of [γ-^{32}P]GTP and 1 mM cGMP. GTPase measurements were conducted for only 3 s to minimize further cGMP dissociation during the measurement. The measurements with GTP/cGMP mixture provide a control that shows that the rate of slow GTPase remains constant during the course of this experiment. The major observation of this experiment is that the extent of the noncatalytic site occupancy by cGMP precisely corresponds to the extent of the transition of transducin GTPase between slow and fast rates. Both processes were described by single exponents: the rate constant for cGMP dissociation was 0.0030 ± 0.0002 s^{-1} (n = 4), while the rate constant for the transition between slow and fast GTPase was 0.0031 ± 0.0008 s^{-1} (n = 4). This coincidence indicates that there is no substantial delay

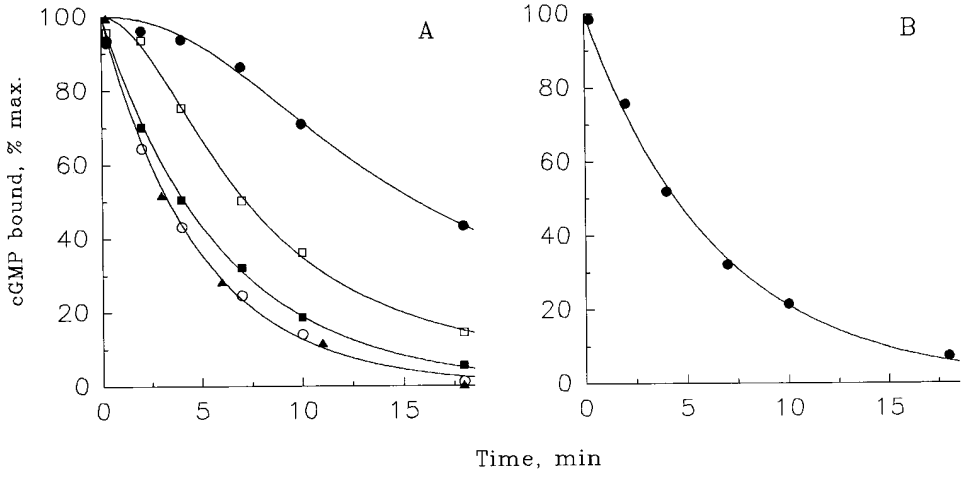

FIGURE 5. cGMP dissociation from the PDE noncatalytic sites after chase with CaM/CaM-PDE (*A*) or excess cGMP (*B*). Suspensions of frog ROS (30 μM rhodopsin) were preincubated for 1 min in pseudointracellular medium containing 50 μM Ca^{2+} and 3 μM [^{3}H]cGMP, and then [^{3}H]cGMP dissociation from the PDE noncatalytic sites was initiated at time zero by a chase with either CaM/CaM-PDE (80 activity units CaM per unit CaM-PDE) or 2 mM nonlabeled cGMP. The amounts of [^{3}H]cGMP bound to PDE were determined as described in METHODS. CaM-PDE concentrations (U/liter): ●, none; □, 7.5; ■, 37; ▲, 150; ○, 740. The data from two lower curves of *A* and the curve in *B* are single exponential fits. The rest of the curves are hand drawn. The figure is representative of three similar experiments.

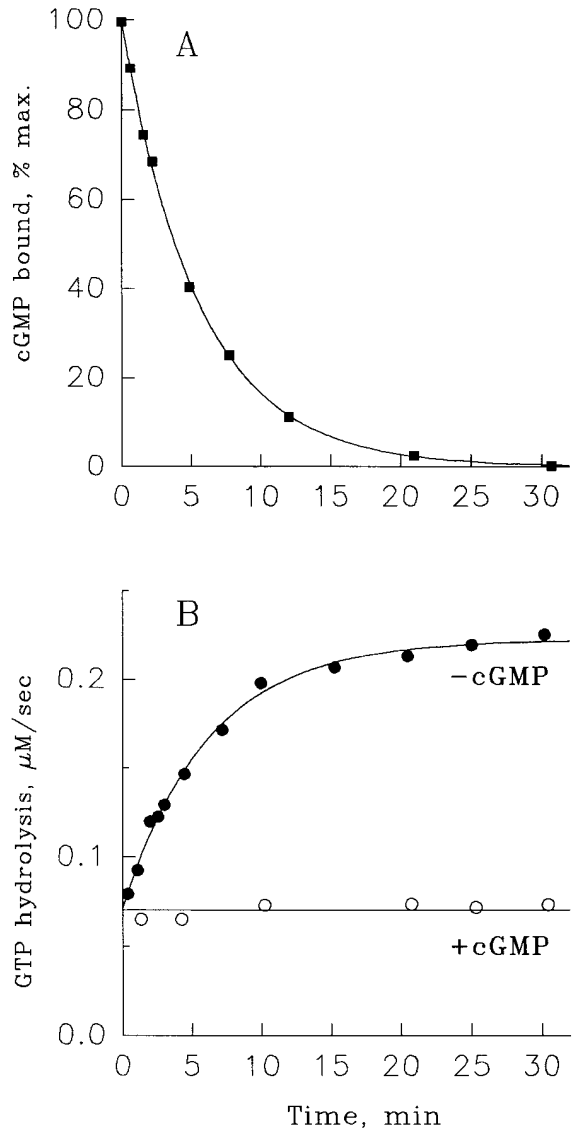

FIGURE 6. Correlation between cGMP dissociation from the PDE noncatalytic sites (*A*) and the transition between slow and fast transducin GTPase (*B*). 600 μl of a ROS suspension containing 30 μM rhodopsin was incubated for 1 min with 3 μM [^{3}H]cGMP, and then a CaM/CaM-PDE mixture (16,000 U/liter CaM, 200 U/liter CaM-PDE) was added at time zero. The amounts of cGMP bound to PDE (*A*) were determined in 15-μl aliquots of the reaction mixture and the rates of transducin GTPase (*B*) were determined in 20-μl aliquots at indicated times as described in methods. GTPase activity was monitored either with the addition of 4 μM [γ-^{32}P]GTP alone (●) or with a mixture of 4 μM [γ-^{32}P]GTP and 1 mM cGMP (○). The rate constant for cGMP dissociation, determined by fitting a single exponential to the data, was 0.0029 s^{-1}. The rate constant for the GTPase transition from slow to fast was also determined by a fit of the data to a single exponential process and found to be 0.0027 s^{-1}. The GTPase rate when cGMP was added with the GTP was constant (*lower curve* in *B*) and was fit with a horizontal line. The figure is representative of four similar experiments.

between dissociation of cGMP from the noncatalytic binding sites and the onset of fast transducin GTPase. Further, the correspondence of the extent of cGMP dissociation with the extent of GTPase activation indicates that each PDE noncatalytic site plays an equal role in regulating transducin GTPase.

cGMP dissociation from the noncatalytic sites of activated PDE after a rapid reduction of free cGMP. Having established that the increase in transducin GTPase directly follows the dissociation of cGMP from the PDE noncatalytic sites, we wanted to know how fast cGMP might dissociate from these sites during the photoreceptor light response. The dissociation rate derived from the data presented in Fig. 5 gives only a slower limit for this process because PDE activation by transducin results in an accelerated rate of cGMP dissociation from the noncatalytic sites (Yamazaki et al., 1982, 1996; Cote et al., 1994). In Fig. 7, we compare the rates of cGMP dissociation from the noncatalytic sites of activated and nonactivated PDE after a chase with CaM/CaM-PDE. As reported earlier (Cote and Brunnock, 1993; Cote et al., 1994; Yamazaki et al., 1996) and as shown above in Fig. 5, cGMP dissociation from nonactivated PDE is a single exponential process, while cGMP dissociation from transducin-activated PDE is biphasic. cGMP dissociates from 32 ± 7% of the sites with a rate constant of 0.11 ± 0.04 s^{-1} and from 68 ± 7% with a rate constant of 0.006 ± 0.001 s^{-1} (n = 5). These rates are at least threefold faster than those obtained by Cote et al. (1994) after a chase with an excess of unlabeled cGMP. A reasonable explanation for this difference is provided by Yamazaki et al. (1996), who suggested that cGMP release from the noncatalytic sites of activated PDE may be inhibited by high concentrations of cGMP. Cote et al. (1994) and Yamazaki et al. (1996) proposed that the biphasic cGMP dissociation is due to a heterogeneity in the noncatalytic cGMP binding sites. However, the mechanism may be different considering that the maximal high affinity cGMP binding observed in our experiments corresponds to two cGMP molecules per PDE holoenzyme, while the amplitudes of the two phases of cGMP dissociation are twofold different rather than being equal as expected.

A chase with GTPγS in the absence of CaM-PDE (Fig. 7, *middle curve*) results in cGMP dissociation kinetics that are only slightly slower than when both GTPγS and CaM/CaM-PDE are included in the chase. 34 ± 7% of the cGMP dissociates with a rate of 0.08 ± 0.02 s^{-1} and 66 ± 7% of cGMP dissociates with a rate of 0.005 ± 0.001 s^{-1} (n = 3). This is in good agreement with the data of Yamazaki et al. (1996) obtained under similar conditions. The virtual coincidence of the cGMP dissociation rate from activated PDE in the presence and absence of CaM/CaM-PDE indicates that when cGMP is present in the physiological concentration range (sev-

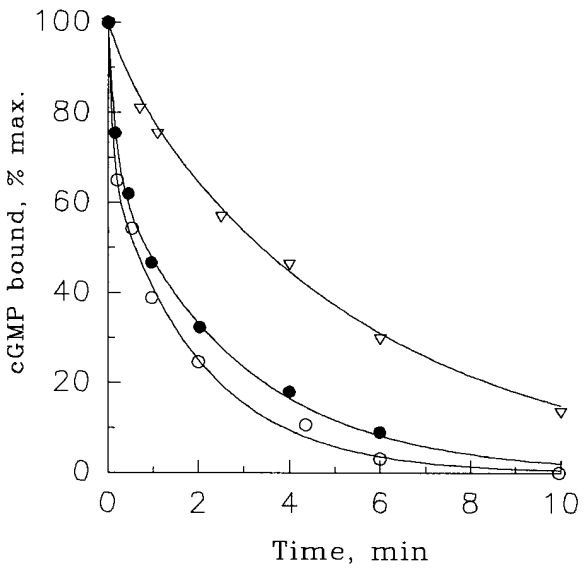

FIGURE 7. Time window for the onset of fast transducin GTPase after bright illumination. Suspensions of bleached ROS (30 μM rhodopsin) were preincubated for 1 min with 3 μM [^{3}H]cGMP. cGMP dissociation from the PDE noncatalytic sites was initiated at time zero by a chase with CaM/CaM-PDE (80,000 U/liter CaM, 1,000 U/liter CaM-PDE) alone (▽), CaM/CaM-PDE with 20 μM GTPγS (○), or with 20 μM GTPγS alone (●). The amounts of [^{3}H]cGMP bound to PDE were determined as described previously. A single exponential process was fit to the data for nonactivated PDE yielding a rate constant of 0.0033 s^{-1}. The data for the dissociation of cGMP from activated PDE with and without the CaM/CaM-PDE chase were each approximated with the sum of two exponential processes. In the case where CaM/CaM-PDE was included in the chase, cGMP dissociated from 33% of the sites with a rate constant of 0.170 s^{-1} and from 67% of the sites with a rate constant of 0.0082. In the case where the chase was initiated with GTPγS alone, cGMP dissociated from 33% of the sites with a rate constant of 0.095 s^{-1} and from 67% of the sites with a rate constant of 0.0058 s^{-1}. The figure is representative of three similar experiments.

eral micromolar), the probability of its being hydrolyzed by activated PDE is higher than the probability of its rebinding to its noncatalytic sites.

DISCUSSION

Ca^{2+} Feedback on Guanylate Cyclase

In the experiments reported in this study, guanylate cyclase activity quickly increases to its maximum after a reduction of the Ca^{2+} concentration with a time constant of ~200 ms (Fig. 3 *A*). With this parameter, and knowing the $K_{1/2}$ and the Hill coefficient for the Ca^{2+}-dependent regulation of cyclase from Fig. 1, we can predict the time course of the increase in cyclase activity as a result of the light-dependent Ca^{2+} reduction in bullfrog ROS. For this analysis, we chose to use a 10-fold regulation of the cyclase by Ca^{2+}, the largest extent of regulation directly observed in our experiments and the lower limit of this parameter in intact cells (see Fig. 2). The analysis is based on the time course of the light-dependent Ca^{2+} reduction in bullfrog ROS cytoplasm as measured by McCarthy et al. (1996). Ca^{2+} declines as the sum of three exponential processes as depicted in Fig. 8 *A*, where the Ca^{2+} concentration is expressed as a percentage of dark Ca^{2+} concentration. Some ambiguity remains as to the actual value of Ca^{2+} concentration in the dark. McCarthy et al. (1996) suggest that the dark Ca^{2+} concentration is within the range of 200–400 nM, so we performed separate analyses using each of these values. The predicted time courses for the onset of the cyclase are shown in Fig. 8 *B,* where a 200-ms delay between the change in Ca^{2+} and the change in the cyclase rate has been imposed. It is seen that the range of the cyclase activity change is highly dependent on the value for the dark Ca^{2+} concentration. A 2.6-fold increase in cyclase activity is observed when the dark Ca^{2+} is assumed to be 400 nM, whereas only a 1.5-fold increase is observed with 200 nM dark Ca^{2+}. We favor the higher value of free dark Ca^{2+} concentration for two reasons. First, it uses more of the dynamic range of cyclase regulation. A value for $K_{1/2}$ (255 nM, Fig. 1) that is higher than the dark Ca^{2+} level will preclude a regulation of the cyclase from being more than twofold, while physiological data (see below) argue for a larger extent of regulation. Second, it is consistent with the estimates of the dark ROS Ca^{2+} concentration in other lower vertebrates: 410 nM from Lagnado et al. (1992) and 534 nM from Sampath et al. (1997) for salamander, and 550 nM from Gray-Keller and Detwiler (1994) for gecko. Importantly, our analysis reveals that the changes in the cyclase activity after a saturating light occur slightly faster than the changes in free Ca^{2+}. The cyclase rate increases 90% within ~5 s, whereas a 90% decrease in Ca^{2+} occurs in ~10 s. This is because the Ca^{2+} dependence of the cyclase is cooperative and the half-saturating Ca^{2+} concentration is close to the dark Ca^{2+} level. It should be noted that our analysis is based on the spatially averaged Ca^{2+} concentration changes in ROS (McCarthy et al., 1996) and, therefore, should be considered as a spatially averaged change in the cyclase rate.

It is interesting to compare our biochemical analysis of guanylate cyclase regulation with indirect estimates obtained using physiological techniques (a more detailed discussion on this topic may be found in a recent review by Pugh et al., 1997). The first physiological measurements of the light-dependent increase in cyclase activity were reported by Hodgkin and Nunn (1988) in salamander rods. By monitoring the rates of the photo-sensitive current rise after suddenly inhibiting PDE by IBMX (3-isobutyl-1-methylxanthine), they estimated the maximum increase to be ~10-fold (Fig. 15 from Hodgkin and Nunn, 1988). A smaller value of six-fold was later reported by Cornwall and Fain (1994).

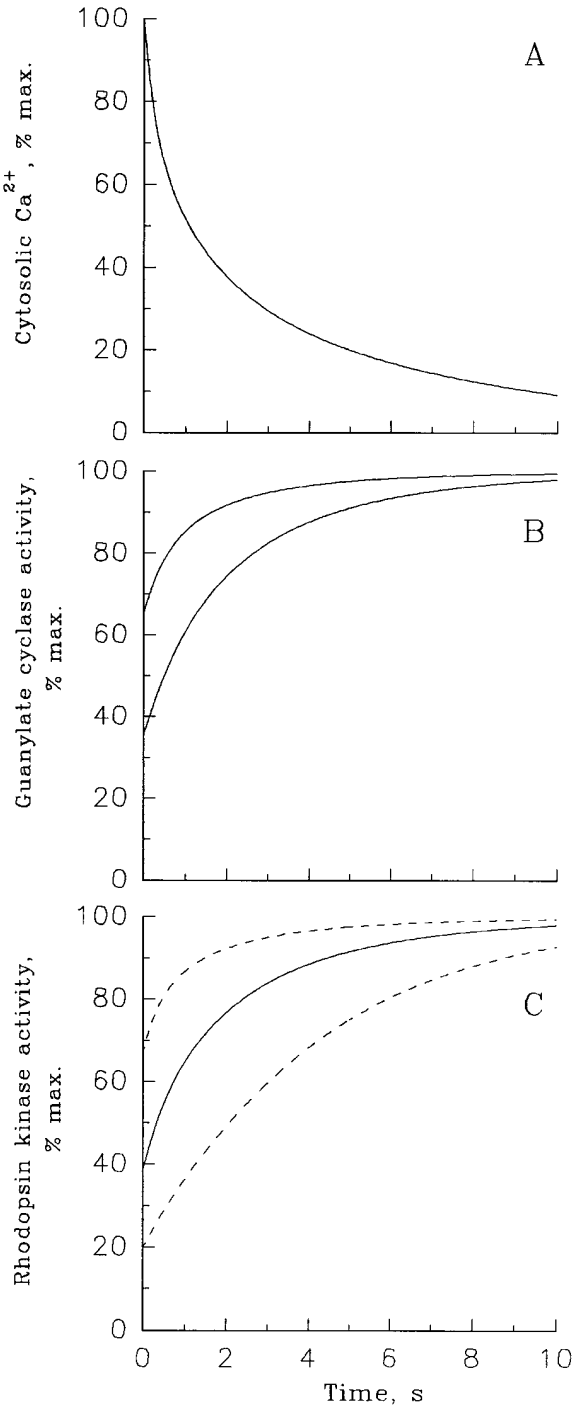

FIGURE 8. Predicted onset of Ca^{2+}-dependent feedback reactions after bright illumination of frog photoreceptors. The time course of Ca^{2+} decline and the predicted increases in guanylate cyclase and rhodopsin kinase activities in rod photoreceptors after exposure to bright illumination is shown. (*A*) Change in free Ca^{2+} after saturating light. The curve was calculated from the sum of three exponential processes (McCarthy et al., 1996): $Ca^{2+}(t) = 25e^{-t/0.25} + 35e^{-t/1.35} + 40e^{-t/6.75}$. (*B*) The onset of the cyclase activity. Cyclase activity was calculated by the numerical solution of this equation and Eq. 1 in the text using the computer program Mathcad (version 6.0; MathSoft, Inc., Cambridge, MA). A 0.2-s delay was imposed between the Ca^{2+} decline and the change in the cyclase rate. The upper curve was calculated assuming a dark Ca^{2+} level of 200 nM and the lower curve with a dark Ca^{2+} of 400 nM. (*C*) Onset of rhodopsin kinase activity. In this case, the delay of 0.11 s found in Fig. 4 was imposed. The Ca^{2+} dependence of the kinase activity was taken from calculations in Klenchin et al. (1995). The solid line assumes a Ca^{2+} $K_{1/2}$ for kinase regulation of 270 nM. The dashed lines above and below the solid line assume Ca^{2+} $K_{1/2}$ values of 540 and 135 nM, respectively.

To the contrary, Koutalos et al. (1995*a*) made indirect measurements of the Ca^{2+} dependence of cyclase activity in truncated salamander ROS and concluded that the maximal extent of the light-dependent cyclase activation is ~30-fold (assuming 400 nM as the dark Ca^{2+} concentration). This difference may be explained by the fact that Koutalos et al. (1995*a*) measured the cyclase activity at high Ca^{2+} to be zero. In fact, their cyclase measurements had a resolution of 1–2 μM/s (Y. Koutalos, personal communication). Thus, in their experiments, enzymatic rates below ~2 μM/s may have been indistinguishable from zero and the actual high Ca^{2+} rate may have been anywhere from zero to 2 μM/s. If we assume that the cyclase rate at high Ca^{2+} was the same as the rate we measured in frogs at the highest ROS concentration, ~1 μM/s, then the dynamic range of cyclase activation measured by Koutalos et al. (1995*a*) would be approximately ninefold, in agreement with others. This activation level is also consistent with the estimates by Dawis et al. (1988) who have found that bright light causes an 8- to 10-fold increase in the cGMP metabolic flux rate in toad retinas.

The at least 10-fold range of guanylate cyclase regulation by Ca^{2+} reported in this study (Fig. 2) is well consistent with the 6–10-fold dark–light difference predicted from the physiological studies. However, the actual range of cyclase stimulation by light calculated in Fig. 8 *B* is only 2.6-fold. We propose three simple explanations for this discrepancy. First, the high/low Ca^{2+} ratio of the cyclase activity in intact photoreceptors should be greater than the 10-fold that we were able to measure in Fig. 2 *B*. Second, it is possible that the actual Ca^{2+} concentration in a dark adapted frog ROS is higher than the 400 nM value used in the calculations. This would allow cyclase to operate over a larger portion of its dynamic range. Third, it is possible that the $K_{1/2}$ value for the Ca^{2+} regulation of cyclase in frog is higher than in salamander. Indeed, while we observe a $K_{1/2}$ of 255 nM in frog, Koutalos et al. (1995*a*) report a $K_{1/2}$ value of 87 nM in salamander. Assuming that the dark Ca^{2+} levels in frog and salamander are similar and equal to ~400 nM, then the light-dependent range of the cyclase activation covers practically the entire Ca^{2+}-dependent range in salamander, whereas only a portion of the Ca^{2+}-dependent range is used by frogs. Another important consequence of the position of the $K_{1/2}$

for Ca^{2+}-dependent cyclase regulation relative to the Ca^{2+} concentration in the dark is that it determines the rate of increase in the cyclase activity upon illumination. The estimates by Hodgkin and Nunn (1988; see Fig. 12) indicate that the halftime of cyclase activation in saturating light is at least 5 s, slower than the 2 s estimated in Fig. 8 *B*. This is consistent with the possibility that the $K_{1/2}$ value for the Ca^{2+} regulation of cyclase in salamander is lower than in frog, while values for dark Ca^{2+} concentrations are similar. However, it could also reflect an artifact of cyclase estimates by their method at high light levels.

Ca^{2+} Feedback on Rhodopsin Kinase

Our study shows that rhodopsin kinase activity also increases practically without delay after a sudden drop in Ca^{2+}. The predicted time course of kinase activation after the onset of saturating light is less straightforward than for guanylate cyclase due to an uncertainty in the Ca^{2+} range for kinase regulation by Ca^{2+} recoverin in vivo. All recent measurements performed in suspensions of disrupted ROS or in reconstituted systems indicate that the half-maximal Ca^{2+} concentration for the rhodopsin kinase regulation by recoverin is above the Ca^{2+} range in intact rods (Klenchin et al., 1995; Chen et al., 1995; Ames et al., 1995). However, physiological experiments performed with recoverin knock-out mice (Dodd et al., 1995) strongly support the idea that the Ca^{2+}-dependent regulation of rhodopsin kinase occurs over the physiological range of Ca^{2+} concentration changes: rods lacking recoverin have accelerated photoresponse recovery and are less able to adapt to light. Two complementary arguments provide a possible resolution of this paradox. First, Zozulya and Stryer (1992) argued that Ca^{2+}-recoverin binding to ROS membranes increases the Ca^{2+} binding affinity to recoverin. Second, Klenchin et al. (1995) have pointed out that because the amount of recoverin in ROS is larger than the amount of rhodopsin kinase, Ca^{2+} binding to a relatively small fraction of recoverin might be sufficient for inhibition of a relatively large fraction of kinase. This results in a lower $K_{1/2}$ for the Ca^{2+}-dependent regulation of kinase than the $K_{1/2}$ for Ca^{2+} binding to recoverin. Klenchin et al. (1995) used both of these arguments to calculate a $K_{1/2}$ of ~270 nM for the Ca^{2+}-dependent kinase regulation in vivo and a maximum extent of the regulation between high and low Ca^{2+} of ~10-fold. Based on these numbers, the value of 400 nM for Ca^{2+} concentration in the dark and our observation that the kinase activity senses the decrease in Ca^{2+} with a delay of ~100 ms, we predicted the time course for the increase in the kinase activity after the onset of saturating illumination (Fig. 8 *C*, *solid curve*). The onset of rhodopsin kinase activation in this case is very similar to the onset of the guanylate cyclase.

An important question raised in our study is why the photoreceptor has two Ca^{2+}-dependent feedback mechanisms, both designed to sense changes in Ca^{2+} quickly. If the Ca^{2+} $K_{1/2}$ values for these mechanisms are indeed close as we discussed above, then their coincidence simply allows the photoreceptor to enhance the amplitude of the Ca^{2+} feedback regulation. If, however, the actual Ca^{2+} $K_{1/2}$ value for rhodopsin kinase is different from that for cyclase, then a temporal hierarchy between two Ca^{2+}-dependent mechanisms is established in addition to an enhanced amplitude. To illustrate this point, we calculated the putative time course of rhodopsin kinase activation for the cases when the value for Ca^{2+} $K_{1/2}$ is twice smaller and twice larger than predicted by Klenchin et al. (1995) (Fig. 8 *C*, *dashed curves*). A higher $K_{1/2}$ value makes the kinase feedback work faster than the cyclase feedback; however, its amplitude is small. Conversely, a lower $K_{1/2}$ value makes the kinase feedback work slower than the cyclase feedback, but its amplitude becomes large. Further clarification of this issue requires a precise determination of the Ca^{2+} $K_{1/2}$ value for the kinase feedback in vivo.

Unlike the case with guanylate cyclase, measurements of the Ca^{2+} $K_{1/2}$ for rhodopsin kinase feedback regulation based on electrophysiological techniques are not available. The closest estimates are provided by Koutalos et al. (1995*b*), who measured the Ca^{2+} dependence of PDE activation by light in truncated salamander rods. They reported a value of 400 nM for the Ca^{2+} $K_{1/2}$. A possible complication of their analysis is that they likely measured a combination of two Ca^{2+} effects on the PDE activation: the effect mediated through rhodopsin kinase and the effect on the rate of transducin activation by photoexcited rhodopsin originally described by Lagnado and Baylor (1994). A subsequent study by Sagoo and Lagnado (1997) indicates that this second Ca^{2+} effect is based on the reduction in the affinity of transducin for GTP upon transducin activation by rhodopsin. A K_m of 9 μM GTP was observed at high Ca^{2+} and 170 μM GTP at low Ca^{2+} while the V_{max} remained unchanged. Since the GTP concentration in intact amphibian rods remains in the millimolar range at any level of illumination (Biernbaum and Bownds, 1985*b*), this mechanism is unlikely to be physiological. The individual impact of rhodopsin kinase regulation and the modulation of transducin activation rate on the overall Ca^{2+} regulation of PDE activation measured by Koutalos et al. (1995*b*) may be distinguished by performing the analysis with millimolar GTP levels rather than with the 100 μM GTP used by these authors.

cGMP Feedback on Transducin GTPase

As opposed to the relatively fast Ca^{2+} dissociation from corresponding binding sites, the dissociation of cGMP from the PDE noncatalytic sites is a slow process with a

rate that is dependent on whether or not PDE is activated by transducin. Since we have demonstrated that cGMP dissociation from these sites results in the immediate acceleration of transducin GTPase, the upper and lower curves from Fig. 7 represent the slowest and fastest limits for the onset of fast GTPase. Two hypotheses for the role of cGMP dissociation from noncatalytic binding sites on PDE are discussed in the literature. Yamazaki et al. (1996) suggested that cGMP dissociation from the noncatalytic sites of activated PDE contributes to cGMP restoration during the recovery phase of the photoresponse, while Cote et al. (1994) proposed that cGMP dissociation contributes to photoreceptor light adaptation to bright continuous light through the acceleration of transducin GTPase. We favor the hypothesis by Cote et al. (1994) for two reasons.

First, the amount of cGMP dissociating from the noncatalytic sites of activated PDE during the time frame of the photoresponse does not appear to be sufficient for significant restoration of hydrolyzed cGMP. Indeed, given the frog rod PDE K_m ~100 μM, V_{max} ~4,000 s^{-1} (Dumke et al., 1994) and free cGMP concentration in darkness ~4 μM (Pugh and Lamb, 1993), ~150 cGMP molecules are hydrolyzed by each activated PDE during the frog rod photoresponse. Yet the data presented in Fig. 7 (virtually the same as in Fig. 4 *B* from Yamazaki et al., 1996) indicate that only ~0.25 cGMP molecules per activated PDE can dissociate from the noncatalytic sites over the time period of four seconds, enough time for complete photoresponse recovery.

Second, the hypothesis that cGMP dissociation from the noncatalytic sites contributes to the speeded recovery of the photoresponse during prolonged bright background illumination is consistent with electrophysiological measurements of Coles and Yamane (1975) and Cervetto et al. (1984). These authors reported a gradual acceleration of photoresponse recovery in amphibian rods after exposure to bright background illumination for tens of seconds. This time scale is substantially slower than the reduction in intracellular Ca^{2+} (McCarthy et al., 1994, 1996; Sampath et al., 1997), indicating that this effect is unlikely to be mediated by Ca^{2+}. A goal of our future experiments is to directly correlate this physiological phenomenon with the occupancy of the noncatalytic cGMP binding sites of frog rod PDE.

We thank Drs. M. Deric Bownds and Victor I. Govardovskii for many helpful discussions, Dr. Clint L. Makino for critically reading the manuscript, and Dr. Elina R. Nekrasova and Mr. Jason Handy for assistance in rapid kinetics experiments.

This work was supported by National Institutes of Health grant EY-10336 and a grant from the Massachusetts Lions Eye Research Foundation Inc. to V.Y. Arshavsky. V.Y. Arshavsky is a recipient of a Jules and Doris Stein Professorship from Research to Prevent Blindness Inc.

Original version received 12 August 1997 and accepted version received 31 October 1997.

REFERENCES

Ames, J.B., T. Porumb, T. Tanaka, M. Ikura, and L. Stryer. 1995. Amino-terminal myristoylation induces cooperative calcium binding to recoverin. *J. Biol. Chem.* 270:4526–4533.

Aparicio, J.G., and M.L. Applebury. 1996. The photoreceptor guanylate cyclase is an autophosphorylating protein kinase. *J. Biol. Chem.* 271:27083–27089.

Arshavsky, V.Y., and M.D. Bownds. 1992. Regulation of deactivation of photoreceptor G protein by its target enzyme and cGMP. *Nature.* 357:416–417.

Arshavsky, V.Y., C.L. Dumke, and M.D. Bownds. 1992. Non-catalytic cGMP binding sites of amphibian rod cGMP phosphodiesterase control interaction with its inhibitory gamma-subunits—a putative regulatory mechanism of the rod photoresponse. *J. Biol. Chem.* 267:24501–24507.

Arshavsky, V.Y., M.P. Gray-Keller, and M.D. Bownds. 1991. cGMP suppresses GTPase activity of a portion of transducin equimolar to phosphodiesterase in frog rod outer segments. Light-induced cGMP decreases as a putative feedback mechanism of the photoresponse. *J. Biol. Chem.* 266:18530–18537.

Biernbaum, M.S., B.M. Binder, and M.D. Bownds. 1991. Dim background light and Cerenkov radiation from ^{32}P block reversal of rhodopsin phosphorylation in intact frog retinal rods. *Visual Neurosci.* 7:499–503.

Biernbaum, M.S., and M.D. Bownds. 1985*a*. Frog rod outer segments with attached inner segment ellipsoids as an in vitro model for photoreceptors on the retina. *J. Gen. Physiol.* 85:83–105.

Biernbaum, M.S., and M.D. Bownds. 1985*b*. Light-induced changes in GTP and ATP in frog rod photoreceptors. Comparison with recovery of dark current and light sensitivity during dark adaptation. *J. Gen. Physiol.* 85:107–121.

Bownds, D., A. Gordon-Walker, A.-C. Gaide-Huguenin, and W. Robinson. 1971. Characterization and analysis of frog photoreceptor membranes. *J. Gen. Physiol.* 58:225–237.

Bownds, M.D., and V.Y. Arshavsky. 1995. What are the mechanisms of photoreceptor adaptation. *Behav. Brain Sci.* 18:415–424.

Brooks, S.P., and K.B. Storey. 1992. Bound and determined: a computer program for making buffers of defined ion concentrations. *Anal. Biochem.* 201:119–126.

Cervetto, L., V. Torre, E. Pasino, P. Marroni, and M. Capovilla. 1984. Recovery from light-desensitization in toad rods. *In* Photoreceptors. A. Borcellino and L. Cervetto, editors. Plenum Press, Inc. New York. 159–175.

Chabre, M., and P. Deterre. 1989. Molecular mechanism of visual transduction. *Eur. J. Biochem.* 179:255–266.

Chen, C.-K., J. Inglese, R.J. Lefkowitz, and J.B. Hurley. 1995. Ca^{2+}-dependent interaction of recoverin with rhodopsin kinase. *J. Biol. Chem.* 270:18060–18066.

Coccia, V.J., and R.H. Cote. 1994. Regulation of intracellular cyclic GMP concentration by light and calcium in electropermeabilized rod photoreceptors. *J. Gen. Physiol.* 103:67–86.

Coles, J.A., and S. Yamane. 1975. Effects of adapting lights on the time course of the receptor potential of the anuran retinal rod. *J.*

Physiol. (Camb.). 247:189–207.

Cornwall, M.C., and G.L. Fain. 1994. Bleached pigment activates transduction in isolated rods of the salamander retina. *J. Physiol. (Camb.).* 480:261–279.

Cote, R.H., M.D. Bownds, and V.Y. Arshavsky. 1994. cGMP binding sites on photoreceptor phosphodiesterase: role in feedback regulation of visual transduction. *Proc. Natl. Acad. Sci. USA.* 91:4845–4849.

Cote, R.H., and M.A. Brunnock. 1993. Intracellular cGMP concentration in rod photoreceptors is regulated by binding to high and moderate affinity cGMP binding sites. *J. Biol. Chem.* 268:17190–17198.

Dawis, S.M., R.M. Graeff, R.A. Heyman, T.F. Walseth, and N.D. Goldberg. 1988. Regulation of cyclic GMP metabolism in toad photoreceptors. *J. Biol. Chem.* 263:8771–8785.

Dizhoor, A.M., C.-K. Chen, E. Olshevskaya, V.V. Sinelnikova, P. Phillipov, and J.B. Hurley. 1993. Role of the acylated amino terminus of recoverin in Ca^{2+}-dependent membrane interaction. *Science.* 259:829–832.

Dizhoor, A.M., and J.B. Hurley. 1996. Inactivation of EF-hands makes GCAP-2 (p24) a constitutive activator of photoreceptor guanylyl cyclase by preventing a Ca^{2+}-induced "activator-to-inhibitor" transition. *J. Biol. Chem.* 271:19346–19350.

Dizhoor, A.M., D.G. Lowe, E.V. Olshevskaya, R.P. Laura, and J.B. Hurley. 1994. The human photoreceptor membrane guanylyl cyclase, RetGC, is present in outer segments and is regulated by calcium and a soluble activator. *Neuron.* 12:1345–1352.

Dizhoor, A.M., E.V. Olshevskaya, W.J. Henzel, S.C. Wong, J.T. Stults, I. Ankoudinova, and J.B. Hurley. 1995. Cloning, sequencing, and expression of a 24-kD Ca^{2+}-binding protein activating photoreceptor guanylyl cyclase. *J. Biol. Chem.* 270:25200–25206.

Dodd, R.L., C.L. Makino, J. Chen, M.I. Simon, and D.A. Baylor. 1995. Visual transduction in transgenic mouse rods lacking recoverin. *Invest. Ophthalmol. Vis. Sci.* 36:S641. (Abstr.)

Dumke, C.L., V.Y. Arshavsky, P.D. Calvert, M.D. Bownds, and E.N. Pugh, Jr. 1994. Rod outer segment structure influences the apparent kinetic parameters of cyclic GMP phosphodiesterase. *J. Gen. Physiol.* 103:1071–1098.

Gillespie, P.G., and J.A. Beavo. 1989. Inhibition and stimulation of photoreceptor phosphodiesterases by dipyridamole and M&B 22,948. *Mol. Pharmacol.* 36:773–781.

Godchaux, W.I., and W.F. Zimmerman. 1979. Membrane-dependent guanine nucleotide binding and GTPase activities of soluble protein from bovine rod cell outer segments. *J. Biol. Chem.* 254:7874–7884.

Gorczyca, W.A., M.P. Gray-Keller. P.B. Detwiler, and K. Palczewski. 1994*a*. Purification and physiological evaluation of a guanylate cyclase activating protein from retinal rods. *Proc. Natl. Acad. Sci. USA.* 91:4014–4018.

Gorczyca, W.A., J.P. Van Hooser, and K. Palczewski. 1994*b*. Nucleotide inhibitors and activators of retinal guanylyl cyclase. *Biochemistry.* 33:3217–3222.

Gray-Keller, M.P., and P.B. Detwiler. 1994. The calcium feedback signal in the phototransduction cascade of vertebrate rods. *Neuron.* 13:849–861.

Hodgkin, A.L., and B.J. Nunn. 1988. Control of light-sensitive current in salamander rods. *J. Physiol. (Camb.).* 403:439–471.

Kawamura, S. 1993. Rhodopsin phosphorylation as a mechanism of cyclic GMP phosphodiesterase regulation by S-modulin. *Nature.* 362:855–857.

Kawamura, S., O. Hisatomi, S. Kayada, F. Tokunaga, and C.-H. Kuo. 1993. Recoverin has S-modulin activity in frog rods. *J. Biol. Chem.* 268:14579–14582.

Klenchin, V.A., P.D. Calvert, and M.D. Bownds. 1995. Inhibition of rhodopsin kinase by recoverin. Further evidence for a negative feedback system in phototransduction. *J. Biol. Chem.* 270:16147–16152.

Koch, K.-W., and L. Stryer. 1988. Highly cooperative feedback control of retinal rod guanylate cyclase by calcium ions. *Nature.* 334: 64–66.

Koutalos, Y., K. Nakatani, T. Tamura, and K.W. Yau. 1995*a*. Characterization of guanylate cyclase activity in single retinal rod outer segments. *J. Gen. Physiol.* 106:863–890.

Koutalos, Y., K. Nakatani, and K.W. Yau. 1995*b*. The cGMP-phosphodiesterase and its contribution to sensitivity regulation in retinal rods. *J. Gen. Physiol.* 106:891–921.

Koutalos, Y., and K.-W. Yau. 1993. A rich complexity emerges in phototransduction. *Curr. Opin. Neurobiol.* 3:513–519.

Lagnado, L., and D. Baylor. 1992. Signal flow in visual transduction. *Neuron.* 8:995–1002.

Lagnado, L., and D.A. Baylor. 1994. Calcium controls light-triggered formation of catalytically active rhodopsin. *Nature.* 367: 273–277.

Lagnado, L., L. Cervetto, and P.A. McNaughton. 1992. Calcium homeostasis in the outer segments of retinal rods from the tiger salamander. *J. Physiol. (Camb.).* 455:111–142.

McCarthy, S.T., J.P. Younger, and W.G. Owen. 1994. Free calcium concentrations in bullfrog rods determined in the presence of multiple forms of Fura-2. *Biophys. J.* 67:2076–2089.

McCarthy, S.T., J.P. Younger, and W.G. Owen. 1996. Dynamic, spatially nonuniform calcium regulation in frog rods exposed to light. *J. Neurophysiol.* 76:1991–2004.

Palczewski, K., I. Subbaraya, W.A. Gorczyca, B.S. Helekar, C.C. Ruiz, H. Ohguro, J. Huang, X. Zhao, J.W. Crabb, R.S. Johnson, et al. 1994. Molecular cloning and characterization of retinal photoreceptor guanylyl cyclase-activating protein. *Neuron.* 13:395–404.

Pugh, E.N., Jr., T. Duda, A. Sitaramayya, and R.K. Sharma. 1997. Photoreceptor guanylate cyclases: a review. *Biosci. Rep.* In press.

Pugh, E.N., Jr., and T.D. Lamb. 1990. Cyclic GMP and calcium: the internal messengers of excitation and adaptation in vertebrate photoreceptors. *Vision Res.* 30:1923–1948.

Sagoo, M.S., and L. Lagnado. 1997. Ca^{2+} increases the apparent affinity of transducin for GTP. *Invest. Ophthalmol. Vis. Sci.* 38:S614. (Abstr.)

Sampath, A.P., H.R. Matthews, M.C. Cornwall, and G.L. Fain. 1997. Bleached pigment produces a maintained decrease in outer segment Ca^{2+} in salamander rods. *Invest. Ophthalmol. Vis. Sci.* 38: S722. (Abstr.)

Woodruff, M.L., and M.D. Bownds. 1979. Amplitude, kinetics, and reversibility of a light-induced decrease in guanosine 3′,5′-cyclic monophosphate in frog photoreceptor membranes. *J. Gen. Physiol.* 73:629–653.

Yamazaki, A., F. Bartucca, A. Ting, and M.W. Bitensky. 1982. Reciprocal effects of an inhibitory factor on catalytic activity and noncatalytic binding sites of rod phosphodiesterase. *Proc. Natl. Acad. Sci. USA.* 79:3702–3706.

Yamazaki, A., V.A. Bondarenko, S. Dua, M. Yamazaki, J. Usukura, and F. Hayashi. 1996. Possible stimulation of retinal rod recovery to dark state by cGMP release from a cGMP phosphodiesterase noncatalytic site. *J. Biol. Chem.* 271:32495–32498.

Yau, K.-W., and D.A. Baylor. 1989. Cyclic GMP-activated conductance of retinal photoreceptor cells. *Annu. Rev. Neurosci.* 12:289–327.

Younger, J.P., S.T. McCarthy, and W.G. Owen. 1996. Light-dependent control of calcium in intact rods of the bullfrog *Rana catesbeiana. J. Neurophysiol.* 75:354–366.

Zozulya, S., and L. Stryer. 1992. Calcium-myristoyl protein switch. *Proc. Natl. Acad. Sci. USA.* 89:11569–11573.